ELSEVIER

Cement & Concrete Composites 25 (2003) 263–276

Cement & Concrete Composites

www.elsevier.com/locate/cemconcomp

Modelling of rectangular RC columns strengthened with FRP

M. Maalej *, S. Tanwongsval, P. Paramasivam

Department of Civil Engineering, The National University of Singapore, 1 Engineering Drive 2, Singapore 117576, Singapore

Received 18 October 2001; accepted 24 April 2002

Abstract

Existing analytical models for predicting the stress–strain or load–displacement response of fibre-reinforced polymer (FRP)-confined concrete are mostly derived for cylindrical plain concrete columns. In practice, however, typical concrete columns come in various shapes including circular, square, or rectangular and incorporate longitudinal and transverse steel reinforcements. Furthermore, strengthening or repairing is typically done while the column is under service loading. In this paper, an analytical model is proposed to predict the load–displacement response of wall-like (i.e. high aspect ratio) reinforced concrete columns strengthened with FRP wraps with and without sustained loading. The model assumes that the general load–displacement response of the strengthened column consists of two distinct branches: a parabolic ascending branch and a linear descending branch. The ascending branch is influenced by the lateral confining pressure from the transverse reinforcement as well as the FRP wraps, while the descending branch is influenced by the buckling of the longitudinal reinforcement and the failure of the core concrete. Comparisons between model results and experimental results indicate close agreement between the two.

Keywords: Axial; Columns; Concrete; FRP; Strengthening; Model

1. Introduction

The introduction of new advanced composite materials in civil engineering has sparked numerous innovative applications. One area in which these lightweight, durable and high strength composite materials have gained popularity is the strengthening and repairing of deficient reinforced concrete structures. Traditionally, the repair or strengthening of reinforced concrete structures such as columns involved a time consuming and disruptive process of removing and replacing the low quality or damaged concrete and/or steel reinforcements with new and stronger material. However, with the introduction of new advanced composite materials such as fibre-reinforced polymer (FRP), concrete columns can now be easily and effectively strengthened by wrapping layers of FRP sheets around the columns. Many researchers [1–4] have shown that circular concrete columns experience a significant increase in strength and ductility when wrapped with FRP sheets. Later studies by Mirmiran et al. [5] and Rochette and Labossiere [6] have shown that the effectiveness of the wraps is dependent on the shape of the column and the stiffness of the FRP wraps. Square- and rectangular-section columns were found to experience less increase in strength and ductility than their circular counterparts. This is because the distribution of lateral confining pressure in circular sections is uniform, in contrast to square and rectangular sections, in which the confining pressure varies from a maximum at the corners to a minimum in between.

The increasing use of FRP to strengthen reinforced concrete columns has outpaced the availability of analytical models and code provisions needed to standardize this technology. Often, the strengthening scheme used are based upon experimental results of strengthened full or laboratory scale models, which can be costly and time consuming. Existing models such as those proposed by Toutanji [1] and Spoelstra and Monti [2] used to predict the stress–strain response were all derived for circular plain concrete columns wrapped with FRP. In practice, however, columns in need of repair or strengthening come in various shapes, including circular, square, or rectangular, and have both longitudinal and transverse steel reinforcements. The applicability of these models to

* Corresponding author. Tel.: +65-6874-4913; fax: +65-6779-1635.
E-mail address: cvemm@nus.edu.sg (M. Maalej).

0958-9465/03/$ - see front matter
PII: S0958-9465(02)00017-3

Nomenclature

A,B,C	contribution of core concrete, the cover concrete and the longitudinal reinforcement to the axial load on the column
A_c	gross cross-sectional area of the column
A_{core}	area of concrete core confined by transverse reinforcement
A_{ie}	ineffectively confined concrete area
A_m	cross-sectional area of external vertical section
A_{sl}	area of longitudinal reinforcement
A_{st}	cross-sectional area of transverse reinforcement
b_c	width of the section where the confining pressure is acting
D	contribution of the FRP wraps to the axial load on the column
d_b	diameter of longitudinal bar
E	contribution of the high strength mortar vertical sections to the axial load on the column
$E_{a\text{-}0}$	tensile modulus of FRP cured laminate in the fibre direction (0°)
$E_{a\text{-}90}$	tensile modulus of FRP cured laminate in the transverse direction (90°)
$E_{ac\text{-}0}$	compressive modulus of FRP cured laminate in the fibre direction (0°)
$E_{ac\text{-}90}$	compressive modulus of FRP cured laminate in the transverse direction (90°)
f'_{cc}	confined concrete peak stress
f'_{co}	unconfined concrete peak stress
f'_{cv}	peak confined concrete cover stress
f_c	stress in the concrete taking into consideration the effect of confinement (12)
f_{cr}^{cn}	compressive stress of confined concrete core of the control column at the level of sustained loading
f_{cr}^{st}	compressive stress of confined concrete core in the strengthened column at the level of sustained loading
f_{cv}^{cn}	compressive stress of confined concrete cover of the control column at the level of sustained loading
f_{cv}^{st}	compressive stress of confined concrete cover in the strengthened column at the level of sustained loading
f_l	uniform lateral confining pressure
f_{la}	lateral confining pressure due to FRP
$f_{la,e}$	effective lateral confining pressure provided by the FRP wraps
$f_{la,ev}$	lateral confining pressure from FRP wraps on concrete cover
f_{le}	effective lateral confining pressure
f_{lex}, f_{ley}	the effective confining pressures perpendicular to core dimensions b_{cx} and b_{cy}, respectively
f_m, f'_{cm}	mortar stress and peak stress, respectively
f_s	longitudinal steel stress
$f_{S/DU}$	longitudinal steel limiting stress
f_{sl}	compressive stress in longitudinal reinforcement as given in (29) or (32)
f_y, f_{sh}, f_u	longitudinal steel yield, strain hardening, and ultimate stress, respectively
f_{yt}	yield stress of transverse reinforcement
g	gauge length of the test region
K	factor amplifying the core concrete peak stress due to lateral confining pressure (11)
k_1, k_2	empirically determined confinement coefficients
k_3	factor accounting for the reduction in average confining pressure in columns with rectangular or square hoops
k_e	confinement effectiveness coefficient
K_v	factor amplifying the cover concrete peak stress due to FRP lateral confining pressure
N	axial load on the column
$N_{la\text{-}0}$	number of FRP cured laminate layers in the fibre direction (0°)
$N_{la\text{-}90}$	number of FRP cured laminate layers in the transverse direction (90°)
P	perimeter of the column
R	radius of the circular transverse reinforcement
r	column's corner radius
R_a	radius of the equivalent transformed circular section

s	spacing of transverse reinforcement
s/d_b	bar aspect ratio
s_l	spacing between the longitudinal reinforcement
t_a	thickness of one FRP cured laminate layer
w	w_x or w_y
w_x	longer dimension of the column
$w_x^2/6$	area of a parabola along the longer dimension
w_y	shorter dimension of the column
$w_y^2/6$	area of a parabola along the shorter dimension
x,y	x, y coordinates of parabolas enclosing the ineffectively confined concrete area
x_l	x-coordinate of the intersection point between parabolas 1 and 2
Δ	axial displacement of the column
ε_{cc}	confined concrete peak strain
ε_{co}	unconfined concrete peak strain
ε_m,ε_{cm}	mortar strain and peak strain, respectively
ε_s	longitudinal steel strain
ε_{20}	strain in the concrete corresponding to the residual stress of 20% of the confined concrete peak stress
$\varepsilon_{S/DU}$	longitudinal steel limiting strain
ε_y,ε_{sh},ε_u	longitudinal steel yield, strain hardening, and ultimate strain, respectively
ε_{85}	axial strain at 85% stress beyond the confined concrete peak stress
ε_a	FRP cured laminate tensile strain
ε_c	axial strain in concrete
ε_{cv}	peak confined concrete cover strain
ε_{sus}	concrete strain corresponding to the sustained loading

FRP-wrapped rectangular reinforced concrete columns would, therefore, be limited. Furthermore, these models do not account for the effect of sustained loading on column repair/strengthening. Normally, and unless steel props are used to transfer the load, columns are subjected to service loads during and after repair. Kaluarachchi [7] reported that when a reinforced concrete column is repaired under sustained service loading, the repair material carries a smaller portion of the applied load when compared to columns repaired without sustained loading. Thus, it is likely that the increase in axial capacity would be less if the columns were strengthened under sustained loading.

This paper presents the results of an analytical model proposed to predict the ultimate load and the complete load–displacement response of strengthened wall-like RC columns taking into account the effect of service loads applied on the column during repair/strengthening. The proposed model should provide a foundation for a better understanding of the behaviour of RC wall-like columns strengthened with FRP wraps and the effects of sustained loading on the strengthening efficiency.

2. Review of previous studies on wall-like RC columns

Neale et al. [8] and Chiew et al., [9] have conducted studies on the strengthening of wall-like RC columns. Both explored the use of glass and carbon composite sheets as well as conventional steel plates as compressive members. Various strengthening schemes were proposed and tested. After a series of trial and error, both agreed that the use of glass-fibre-reinforced polymer (GFRP) was preferable to that of carbon-fibre-reinforced polymer (CFRP), as the former has a thicker section, which offers higher stability against buckling. Finally, both adopted a similar scheme in which thick FRP C-channels were fabricated and attached to the ends of the columns with two horizontal FRP layers wrapped around the columns to prevent the channels from buckling. Test results showed an increase in axial capacity by as much as 33% when eight vertical GFRP layers were used. Although a satisfactory increase in axial capacity was achieved in the study, the test program did not simulate the actual loading conditions of typical columns.

In view of the above limitations, a total of five wall-like reinforced concrete columns (Fig. 1) with dimensions of ≈115 mm in thickness, 420 mm in width, and 1500 mm in height were tested [10]. The material properties and the testing program are summarized in Tables 1 and 2, respectively. The load–displacement curves of the tested columns are given in Fig. 2. As the figure indicates, the load–displacement response consists of two distinct branches: a parabolic ascending branch and a linear descending branch. Consequently, in the analytical model, the response is first considered to consist

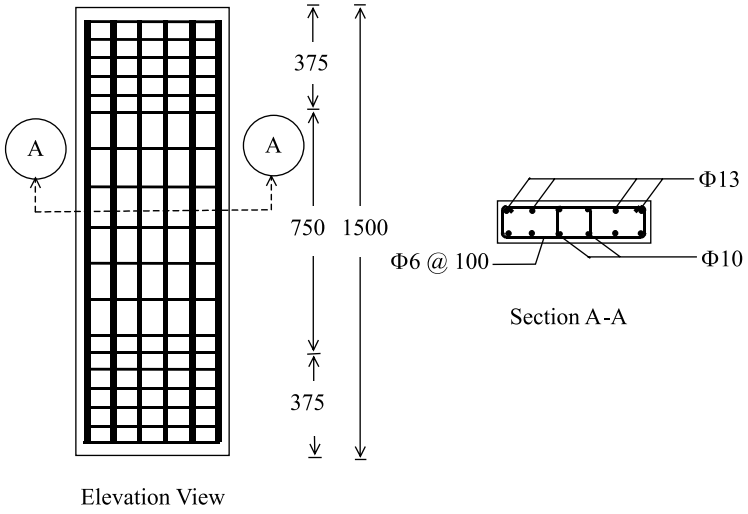

Fig. 1. Reinforcement details of wall-like column.

Table 1
Mechanical properties of materials

Material	Properties
Concrete	$f'_{co} = 32.4$ MPa, $\varepsilon_{co} = 0.002$
Longitudinal reinforcement (T13) $\phi = 13$ mm	$f_y = 461$ MPa, $E_s = 171$ GPa, $f_{sh} = 458$ MPa, $f_u = 561$ MPa, $\varepsilon_{sh} = 0.0234$, $\varepsilon_u = 0.0900$
Longitudinal reinforcement (T10) $\phi = 10$ mm	$f_y = 541$ MPa, $E_s = 186$ GPa, $f_{sh} = 541$ MPa, $f_u = 626$ MPa, $\varepsilon_{sh} = 0.0320$, $\varepsilon_u = 0.0934$
Transverse reinforcement (R6) $\phi = 6$ mm	$f_y = 365$ MPa, $E_s = 211$ GPa
FRP cured laminate tensile properties	$f_{au} = 600$ MPa, $\varepsilon_{au} = 0.0224$, $E_{a\text{-}0} = 26\,130$ MPa, $E_{a\text{-}90} = 6785$ MPa, $t_a = 1.08$ mm
FRP cured laminate compressive properties	$E_{ac\text{-}0} = 26\,789$ MPa, $E_{ac\text{-}90} = 8391$ MPa
Prestressing tendons	$f_{pu} = 1860$ MPa, $E_p = 195$ GPa
High strength repair mortar	$f'_{cm} = 59.5$ MPa, $\varepsilon_{cm} = 0.003$

Table 2
Summary of the test program

Scheme	Schematic representation	Legend	
Control	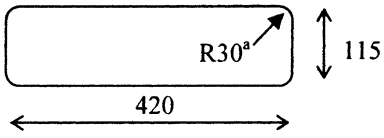		2 vertical GFRP layers
			1 vertical GFRP layer
Scheme 1 (2H2V-NL and 2H2V-L)	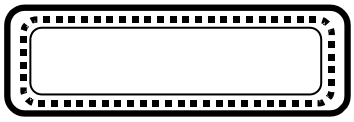		2 horizontal GFRP layers
Scheme 2 (2H-VA-NL and 2H-VA-L)	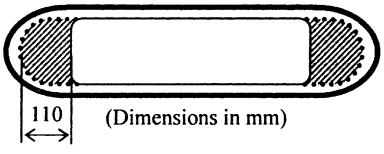		High strength repair mortar

[a]Corner radius.

of two separate branches, which are later combined to obtain the complete load–displacement response.

In the above study, the delamination of the concrete cover and subsequent buckling of the longitudinal rein-

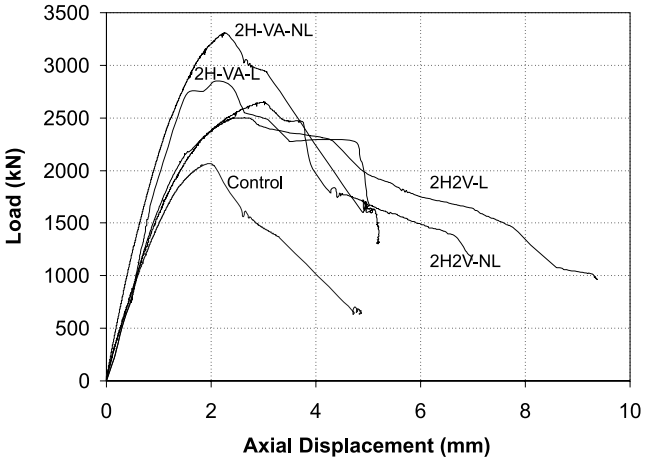

Fig. 2. Load–displacement response of tested columns.

forcement appeared to be the primary cause of failure. The phenomenon was visually observed in the control column and was believed to have controlled the failure of the strengthened columns, judging from the observed bulging of these specimens in the test region at failure (Fig. 3).

3. Existing confined concrete models

The proposed confinement model for reinforced concrete rectangular columns wrapped with FRP is based, in part, upon several models and techniques proposed by various researchers. Thus, it is imperative to discuss the important aspects of the existing models and the reasons why a particular model or technique was selected.

3.1. Steel confined concrete models

The early investigation by Richart et al. [11] on compressive strength testing of concrete cylinders confined under hydrostatic pressure has shown that the confined concrete peak stress and strain can be determined by the following expressions:

$$f'_{cc} = f'_{co} + k_1 f_l \tag{1}$$

$$\varepsilon_{cc} = \varepsilon_{co}\left(1 + k_2 \frac{f_l}{f'_{co}}\right) \tag{2}$$

where f'_{cc} is the confined concrete peak stress, f'_{co} is the unconfined concrete peak stress, f_l is the uniform confining pressure, ε_{cc} is the confined concrete peak strain, ε_{co} is the unconfined concrete peak strain and k_1 and k_2 are empirically determined confinement coefficients.

Furthermore, they reported that the average values of the confinement coefficients k_1 and k_2 obtained from the test data to be 4.1 and $5k_1$, respectively. Saatcioglu and Razvi [12] later found that k_1 had low values at high lateral pressure and could be empirically expressed as:

$$k_1 = 6.7 f_l^{-0.17} \tag{3}$$

Mander et al. [13] proposed a unified stress–strain model based on equations suggested by Popovics [14] to

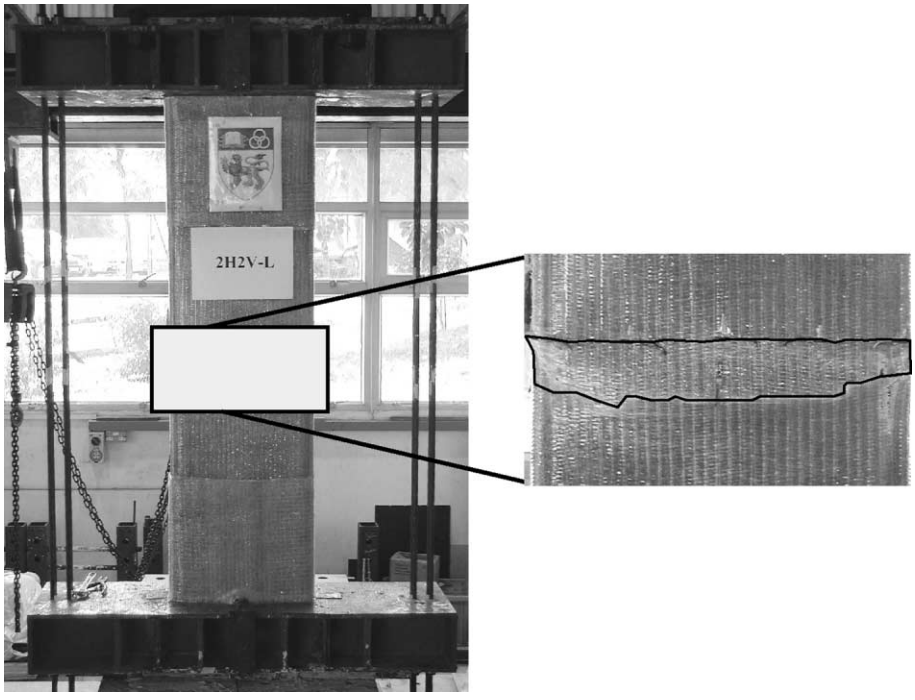

Fig. 3. Typical bulging of the FRP in the test region.

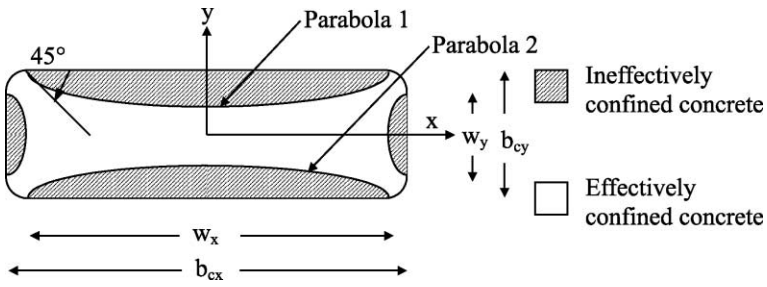

Fig. 4. Effectively confined concrete area.

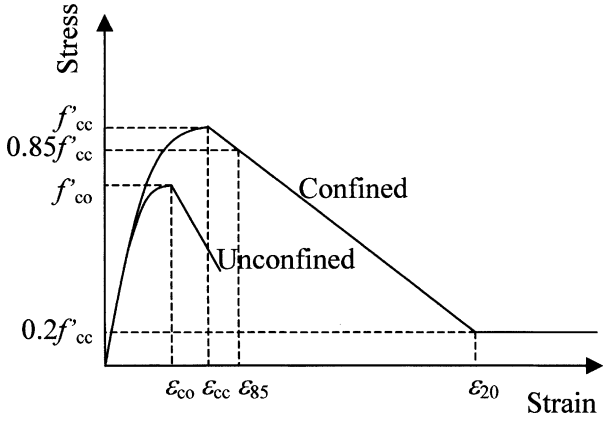

Fig. 5. Stress–strain response of steel-confined concrete.

construct the complete stress–strain response for steel-confined concrete applicable to both circular and rectangular columns under slow strain rate and monotonic loading. The constant effective lateral confining pressure exerted by the transverse reinforcement was determined by an approach similar to the one used by Sheikh and Uzumeri [15]. The effectively confined area was assumed to occur within the region where the arching action had been fully developed. As shown in Fig. 4, the arching action is represented in the form of a second-degree parabola with an initial tangent slope of 45°. The area within the parabolas was considered as ineffectively confined. This approach will later be modified to determine the confining pressure of FRP wraps on a rectangular RC column.

Saatcioglu and Razvi [12] proposed a model to predict the stress–strain response of reinforced concrete columns based on earlier findings by Richart et al., [11] and Hognestad [16]. They noticed that the stress–strain response of confined concrete was comprised of two distinct regions as shown in Fig. 5. Consequently, the parabolic ascending region was represented by a modified Hognestad [16] equation for unconfined concrete under uniaxial load, while the linear descending region was constructed by joining two points corresponding to 85% and 20% stress level beyond the peak stress. A constant residual stress was assumed at 20% of the peak stress. The prediction was later compared to a large experimental database of various types of columns tested under fast and slow strain rates. The results indicated good agreement between the experimental data and the model.

3.2. FRP-confined concrete models

Toutanji [1] divided the stress–strain response of FRP-confined concrete cylinder into two distinct regions. In the first region, the response was similar to that of unconfined concrete with higher peak stress and strain. An equation initially proposed by Ahmad and Shah [17] was modified and used to calculate the stress–strain curve for the first region. In the second region, the FRP wrap became fully activated as the concrete started to disintegrate. Strength and ductility of the concrete cylinder increased significantly. This was in contrast to steel-confined concrete in which only slight increase in strength and ductility was observed. This was due to the inherent difference in the mechanical response between steel and FRP. Steel behaves elastically until yielding after which it behaves plastically, while FRP behaves elastically until failure. Consequently, Toutanji [1] modified expressions (1) and (2) initially proposed by Richart et al., [11] for concrete cylinders confined by hydrostatic pressure to calculate the stress–strain response for the second region.

Spoelstra and Monti [2] employed a different approach in determining the stress–strain curve of FRP-confined concrete cylinder. They proposed an iterative procedure in which the concrete axial strain and lateral confining pressure were initially assumed. Then the confined concrete peak stress was calculated based on equations proposed by Mander et al., [13]. Once the confined peak stress was known, the current concrete stress corresponding to the initially assumed concrete strain was calculated. The constitutive model proposed by Pantazopoulou and Mills [18] was then used to determine the lateral concrete strain corresponding to the current compressive stress. With the lateral strain known, the actual confining pressure on the cylinder can

be determined from equilibrium and boundary conditions. The actual confining pressure was compared to the assumed lateral pressure. If both were similar, a new axial strain and lateral pressure were assumed and the procedure was repeated. Otherwise, the actual confining pressure was used as the next assumed lateral confining pressure and the procedure was repeated.

4. Proposed model

4.1. Ascending branch

The proposed model considered the load–displacement response of unstrengthened and strengthened wall-like reinforced concrete columns to consist of two distinct branches—a parabolic ascending branch and a linear descending branch. The components contributing to the total axial load on the column in the ascending branch include (depending on the column) the core and cover concrete, the longitudinal reinforcements, the FRP wraps, and the external vertical sections. The equations proposed by Saatcioglu and Razvi [12] and Hognestad [16] were used to determine the contribution of the confined concrete core and the unconfined concrete cover to the ascending branch, respectively. The confined concrete model proposed by Saatcioglu and Razvi [12] was chosen to predict the load–displacement response of wall-like RC columns wrapped with FRP because of the model's simplicity as well as its versatility which allows the lateral pressure from different types of reinforcement to be superimposed. Thus, the lateral confining pressure exerted by the FRP wraps can be easily included in the model.

4.1.1. Contribution of the concrete and the reinforcing steel

The lateral confining pressure in Eq. (1) was defined as a uniform confining pressure. For circular steel hoops, the uniform lateral pressure can easily be determined by considering the force equilibrium of the free body diagram of the half circular section:

$$f_l = \frac{A_{st} f_{yt}}{sR} \quad \text{(MPa)} \tag{4}$$

where A_{st}, f_{yt}, s and R are, respectively, the cross-sectional area, the yield stress, the spacing and the radius of the circular transverse reinforcement. Similarly, the lateral confining pressure for rectangular hoops can be determined as:

$$f_l = \frac{\sum A_{st} f_{yt}}{s b_c} \quad \text{(MPa)} \tag{5}$$

where b_c is the width of the section where the confining pressure is acting.

However, for rectangular or square hoops, the confining pressure is not uniform. The maximum confining pressure exists at the corners or locations where it is laterally supported by the longitudinal reinforcement, while minimum pressure exists between the laterally supported corners or locations. Furthermore, the use of an average uniform confining pressure for rectangular or square hoops was found to overestimate the actual confining pressure. Saatcioglu and Razvi [12] proposed a coefficient k_3, which was derived from regression analysis of test data based on the material and geometric properties of the column, to reduce the average confining pressure:

$$k_3 = 0.26\sqrt{\left(\frac{b_c}{s}\right)\left(\frac{b_c}{s_l}\right)\left(\frac{1}{f_l}\right)} \leqslant 1.0 \tag{6}$$

where f_l is the lateral confining pressure as defined in (5) and s_l is the spacing between the longitudinal reinforcement. The reduced or effective uniform confining pressure for a rectangular section is therefore:

$$f_{le} = k_3 f_l \tag{7}$$

Another modification to the effective lateral confining pressure is required when the columns have different confining pressures in the two orthogonal directions. This was common for rectangular sections and sometimes for square sections. From the experimental data, Saatcioglu and Razvi [12] proposed that the different confinement pressures along the two directions might be considered proportional to the cross-sectional dimensions. Thus, the lateral confining pressure can be written as:

$$f_{le} = \frac{f_{lex} b_{cx} + f_{ley} b_{cy}}{b_{cx} + b_{cy}} \tag{8}$$

where f_{lex} and f_{ley} are the effective confining pressures perpendicular to the core dimensions b_{cx} and b_{cy}, respectively. The confined concrete peak stress and strain in Eqs. (1) and (2) can now be written as:

$$f'_{cc} = f'_{co} + k_1 f_{le} \tag{9}$$

$$\varepsilon_{cc} = \varepsilon_{co}(1 + 5K) \tag{10}$$

where

$$K = \frac{k_1 f_{le}}{f'_{co}} \tag{11}$$

With the confined concrete peak stress and strain known, the ascending portion of the stress–strain response can be determined. The stress–strain relationship of steel-confined concrete proposed by Saatcioglu and Razvi [12] was a modified Hognestad [16] equation for unconfined concrete and is given as follows:

$$f_c = f'_{cc}\left[2\left(\frac{\varepsilon_c}{\varepsilon_{cc}}\right) - \left(\frac{\varepsilon_c}{\varepsilon_{cc}}\right)^2\right]^{1/(1+2K)} \leqslant f'_{cc} \tag{12}$$

Finally, the load–displacement response of the ascending branch can be computed by numerically combining the contributions from the core concrete (A), the cover concrete (B) and the longitudinal reinforcement (C) as follows (assuming that $\varepsilon_s = \varepsilon_c$):

$$N = A + B + C \tag{13}$$

$$A = 0.85\left(A_{core} - \sum A_{sl}\right)f'_{cc}\left[2\left(\frac{\varepsilon_c}{\varepsilon_{cc}}\right) - \left(\frac{\varepsilon_c}{\varepsilon_{cc}}\right)^2\right]^{1/(1+2K)} \tag{14}$$

$$B = 0.85(A_c - A_{core})f'_{co}\left[2\left(\frac{\varepsilon_c}{\varepsilon_{co}}\right) - \left(\frac{\varepsilon_c}{\varepsilon_{co}}\right)^2\right] \tag{15}$$

$$C = \sum f_{sl}A_{sl} \tag{16}$$

where N is the axial load on the column, ε_c is the axial strain in the concrete, A_c is the cross-sectional area of the column, A_{core} is the area of the concrete core confined by the transverse reinforcement, A_{sl} is the area of the longitudinal reinforcement, and f_{sl} is the compressive stress in the longitudinal reinforcement as given later in (29) or (32). The axial displacement of the column can be determined by:

$$\Delta = \varepsilon_c g \tag{17}$$

where g is gauge length of the test region.

4.1.2. Contribution of the FRP wraps

The above procedure is applicable to conventional reinforced concrete columns. For columns strengthened with horizontal and vertical FRP wraps, the additional confinement provided by the FRP wraps must be determined and added to the effective lateral confining pressure from the transverse steel reinforcement to obtain the total effective lateral pressure exerted on the core concrete. Also, the contribution of the FRP wraps to the axial load on the column must be included in Eq. (13). In addition, the concrete cover is now confined by the FRP wraps and this must be accounted for when computing the axial load on the column.

Similar to the case of rectangular hoops, the confining pressure exerted on a rectangular RC column by the FRP wraps is not uniform, but maximum at the corners and minimum in between. To determine the effective lateral confining pressure, the rectangular section is transformed into a circular section with an equivalent cross-sectional area as shown in Fig. 6. The horizontal and vertical FRP layers were assumed to wrap around this transformed circular section. The lateral confining pressure can then be determined by considering the free body diagram of the half-circular section. For the purpose of the analytical prediction, the lateral confining pressure contributed by both the horizontal and vertical FRP layers were considered, although the latter has a much lower tensile modulus in the transverse direction (Table 1). From equilibrium, the lateral confining pressure can be determined as follows:

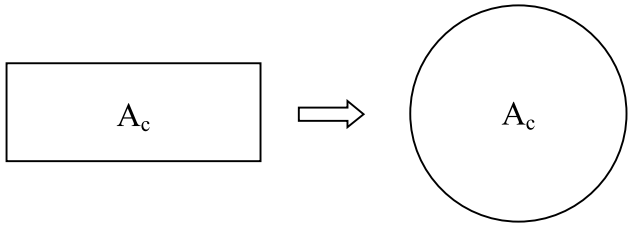

Fig. 6. Transformation of the column's cross section.

$$f_{la} = \frac{(E_{a\text{-}0}N_{la\text{-}0} + E_{a\text{-}90}N_{la\text{-}90})\varepsilon_a t_a}{R_a} \tag{18}$$

where $E_{a\text{-}0}$ and $E_{a\text{-}90}$ are the tensile moduli of the FRP cured laminate in the fibre (0°) and transverse (90°) directions, $N_{la\text{-}0}$ and $N_{la\text{-}90}$ are the numbers of FRP cured laminate layers in the fibre (0°) and transverse (90°) directions, ε_a is the FRP cured laminate tensile strain, t_a is the thickness of one FRP cured laminate layer, and R_a is the radius of the equivalent transformed circular section.

Since the maximum lateral confining pressure provided by the transverse reinforcement is reached when the transverse reinforcement yields, the lateral confining pressure provided by the FRP wraps is assumed to reach a maximum value when the tensile strain in the FRP is equal to the yield strain of the transverse reinforcement. Therefore, Eq. (18) can be written as:

$$f_{la} = \frac{f_{yt}}{E_{st}}\frac{(E_{a\text{-}0}N_{la\text{-}0} + E_{a\text{-}90}N_{la\text{-}90})t_a}{R_a} \tag{19}$$

To determine the effectively confined concrete area, the procedure proposed by Sheikh and Uzumeri [15] is used. As shown in Fig. 4, it is assumed that the ineffectively confined areas are enclosed by second-degree parabolas with an initial tangent slope of 45°. From geometry, the enclosed area can be derived as:

$$\frac{w^2}{6} \tag{20}$$

where w is equal to the column longer or shorter dimension (w_x or w_y), respectively. However, as the aspect ratio increases, the parabolas along the longer dimension (parabola 1 and 2) may overlap. From the boundary conditions, the general equation of Parabolas 1 and 2 can be derived as:

$$y_1 = \frac{1}{w_x}x^2 + \frac{1}{4}(2b_{cy} - w_x) \tag{21}$$

$$y_2 = -\left(\frac{1}{w_x}x^2 + \frac{1}{4}(2b_{cy} - w_x)\right) \tag{22}$$

where w_x is equal to $(b_{cx} - 2r)$ and r is the column's corner radius. Equating (21) to (22) shows that when $2b_{cy} < w_x$, the two parabolas along the longer dimensions will intersect at x equal to x_1. The overlapping area is then deducted from the total ineffectively-confined area as follows:

$$A_{ie} = \sum_{i=1}^{2} 2\int_0^{w_x/2} (-1)^{i+1}\left(\frac{b_{cy}}{2} - y_i\right)dx + 2\frac{w_y^2}{6} - 2\int_0^{x_1}(y_2 - y_1)\,dx \tag{23}$$

After the ineffectively confined concrete area is calculated, the confinement effectiveness coefficient k_e and the effective lateral confining pressure $f_{la,e}$ provided by the FRP wraps can be determined as:

$$k_e = \frac{A_c - A_{ie}}{A_c} \tag{24}$$

$$f_{la,e} = k_e f_{la} \tag{25}$$

The effective lateral confining pressure from the FRP can then be simply added to the confining pressure exerted by the steel reinforcement to obtain the total confining pressure on the core concrete. For the concrete cover, however, the confining pressure comes only from the FRP wraps. Finally, the contribution of the FRP wraps (D) to the axial load on the column can be calculated from Eq. (26) and included in Eq. (13):

$$D = (E_{ac\text{-}0}N_{la\text{-}0} + E_{ac\text{-}90}N_{la\text{-}90})Pt_a\varepsilon_c \tag{26}$$

where P is the perimeter of the column and $E_{ac\text{-}0}$ and $E_{ac\text{-}90}$ are the compressive moduli of the FRP cured laminate in the fibre (0°) and transverse (90°) directions, respectively.

4.1.3. Contribution of the external vertical sections

For specimens strengthened with external vertical sections, the contribution of the vertical sections (E) to the axial load on the column is based on Eq. (28), which was obtained by regression analysis of the actual stress–strain response of the high strength mortar (see Fig. 7):

$$E = 2f_m A_m \tag{27}$$

$$\frac{f_m}{f'_{cm}} = -0.564\left(\frac{\varepsilon_m}{\varepsilon_{cm}}\right)^3 + 0.118\left(\frac{\varepsilon_m}{\varepsilon_{cm}}\right)^2 + 1.448\left(\frac{\varepsilon_m}{\varepsilon_{cm}}\right) - 2\times 10^{-5} \tag{28}$$

where A_m is the cross-sectional area of the mortar external vertical section, and f_m, f'_{cm}, ε_m and ε_{cm} are the mortar stress, peak stress, strain and peak strain, respectively.

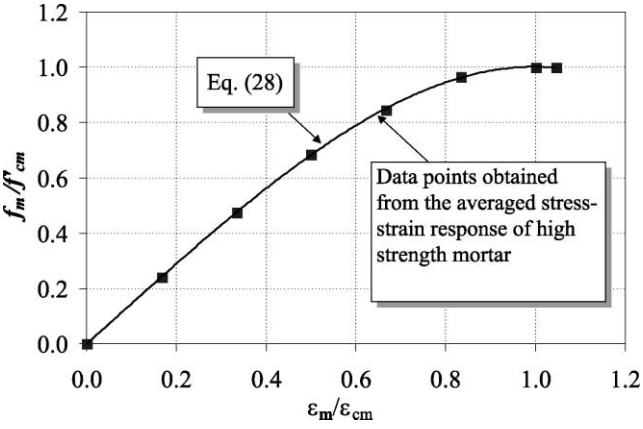

Fig. 7. Normalized stress–strain response of high strength mortar.

Since the mortar in the external vertical sections was confined by the FRP wrap, the peak stress and strain used in Eq. (28) must, therefore, be the confined mortar peak stress and strain, which were determined using Eqs. (9) and (10), respectively. The lateral confining pressure used in Eqs. (9) and (10) was determined from the proposed cross-section transformation methodology and Eq. (19).

4.2. Descending branch

It was observed from the experiment that the control column failed by localized buckling of the longitudinal reinforcement. The final response of the column should, therefore, be governed by the behaviour of the longitudinal reinforcement in compression. Since the observed descending branch was practically a straight line, the branch can be determined by connecting the peak load with the load corresponding to the limiting stress of the longitudinal reinforcement (see Fig. 8). However, with two different sizes of longitudinal reinforcement used, failure was assumed to occur once either size reached its limiting stress.

4.2.1. Contribution of the longitudinal steel reinforcement

The buckling or instability of the longitudinal steel reinforcement is related to the bar aspect ratio (s/d_b),

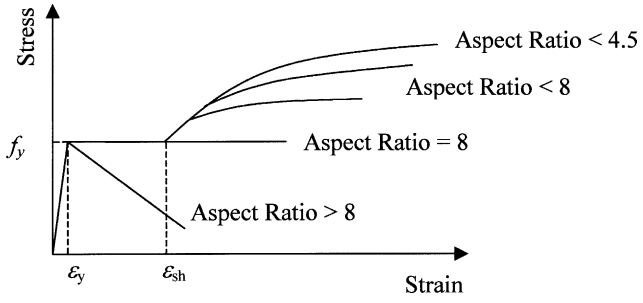

Fig. 8. Stress–strain relationship for reinforcing steel in compression.

which is the ratio of unsupported bar length between two ties to its diameter and the lateral support provided by the concrete cover. If the bar aspect ratio is high, the bar can lose its stability due to buckling prior to developing full strain hardening. The relationship is illustrated in Fig. 8.

When the aspect ratio of the bar is greater than 8.0, the bar becomes unstable at yielding [19]. As shown in Fig. 8, the stress linearly drops until the limiting stress and strain given by Eqs. (30) and (31) are reached. For bars with aspect ratio $\leqslant 8.0$, the response is somewhat similar to that of a bar in tension with a possible strain hardening regime. If the aspect ratio is <4.5, the behaviour becomes identical to that of a bar in tension. Yalcin and Saatcioglu [19] presented the following empirical relationships between the bar aspect ratio and the corresponding compressive stress–strain response:

(a) Aspect ratio $\geqslant 8.0$

$$f_{sl} = f_y - (\varepsilon_s - \varepsilon_y)\left[-23\,000 + 11\,000\ln\left(\frac{s}{d_b}\right)\right]$$

$$\text{for } \varepsilon_y < \varepsilon_s \leqslant \varepsilon_{S/DU} \tag{29}$$

$$f_{S/DU} = 28\left(\frac{s}{d_b}\right)^{-1.7} f_y \tag{30}$$

$$\varepsilon_{S/DU} = \left[40 - 6\ln\left(\frac{s}{d_b}\right)\right]\varepsilon_y \tag{31}$$

(b) Aspect ratio $\leqslant 8.0$

$$f_{sl} = f_y + (f_{S/DU} - f_{sh})\left[2\frac{\varepsilon_s - \varepsilon_{sh}}{\varepsilon_{S/DU} - \varepsilon_{sh}} - \left(\frac{\varepsilon_s - \varepsilon_{sh}}{\varepsilon_{S/DU} - \varepsilon_{sh}}\right)^2\right]$$

$$\text{for } \varepsilon_s > \varepsilon_{sh} \tag{32}$$

$$f_{S/DU} = f_{sh} + (f_u - f_{sh})\left[48e^{-0.9(s/d_b)}\right] \tag{33}$$

$$\varepsilon_{S/DU} = \varepsilon_{sh} + (\varepsilon_u - \varepsilon_{sh})\left[6e^{-0.4(s/d_b)}\right] \tag{34}$$

where f_y, f_{sh}, f_u, $f_{S/DU}$, ε_y, ε_{sh}, ε_u and $\varepsilon_{S/DU}$ are the longitudinal steel yield, strain hardening, ultimate and limiting stresses and strains, respectively.

The contribution of the longitudinal reinforcement to the axial load on the column (Eq. (16)) must, therefore, be computed taking into account the various stress–strain relationships given for steel with different aspect ratios under compression. For the present series of specimens, the critical bar aspect ratio s/d_b is equal to 10 (corresponding to the longitudinal reinforcement with a diameter of 10 mm).

4.2.2. Contribution of the confined concrete/mortar

The minimum contribution of the confined concrete/mortar to the descending branch was assumed as 20% of the confined concrete/mortar peak stress. This was adopted from Saatcioglu and Razvi's [12] assumption that a residual stress equal to 20% of the confined concrete peak stress exists beyond a compressive strain equal to:

$$\varepsilon_{20} = \frac{0.8}{0.15}(\varepsilon_{85} - \varepsilon_{cc}) + \varepsilon_{cc} \tag{35}$$

where ε_{85} is the axial strain at 85% stress beyond the peak (see Fig. 5) given by:

$$\varepsilon_{85} = 260\varepsilon_{cc}\left[\frac{\sum A_{sl}}{s(b_{cx} + b_{cy})}\right] + 0.0038 \tag{36}$$

The total load carried by the column at the limiting strain of the longitudinal steel consists of the confined concrete residual load and the load carried by the longitudinal reinforcements. The axial displacement can be calculated from:

$$\Delta = (\varepsilon_{S/DU} - \varepsilon_{cc})s + \varepsilon_{cc}g \tag{37}$$

The rationale behind using the spacing of the transverse reinforcement as the gage length to determine the displacement at failure (referring to the first term on the right hand side of Eq. (37)), was that the failure region was assumed to be between two consecutive ties, which was also the unsupported length used to determine the longitudinal reinforcement's aspect ratio.

4.3. Effects of sustained loading

Prior to strengthening, the column's response is theoretically identical to that of the control column and can be determined using Eqs. (13)–(17). After strengthening, however, the equations have to be modified to take into account the losses in the axial load and the FRP-induced confining pressure due to the initial absence of the retrofit material and FRP wraps, respectively.

The loss in the axial load due to the absence of either the FRP wraps or the external vertical sections can easily be considered by reducing the current axial strain by the strain due to sustained loading (ε_{sus}). Consequently, the axial strains ε_c and ε_m in Eqs. (26) and (28) can be replaced by $(\varepsilon_c - \varepsilon_{sus})$ and $(\varepsilon_m - \varepsilon_{sus})$, respectively.

The loss in confining pressure in the core and cover concrete can be determined by considering the difference between the stress level in the core (f_{cr}^{cn}) and the cover (f_{cv}^{cn}) concrete in the control column and the stress level in the core (f_{cr}^{st}) and the cover (f_{cv}^{st}) concrete in the strengthened column at the level of sustained loading. This difference should correspond to the stress lost due to sustained loading and must be deducted from the total stress in the core and cover concrete. The modified contributions from the core and cover concrete (con-

tributions A and B, respectively) beyond the level of sustained loading are given below:

$$A = 0.85(A_{\text{core}} - \sum A_{\text{sl}}) \times \left(f'_{\text{cc}} \left[2\left(\frac{\varepsilon_{\text{c}}}{\varepsilon_{\text{cc}}}\right) - \left(\frac{\varepsilon_{\text{c}}}{\varepsilon_{\text{cc}}}\right)^2 \right]^{1/(1+2K)} - \left(f^{\text{st}}_{\text{cr}} - f^{\text{cn}}_{\text{cr}}\right) \right) \tag{38}$$

$$B = 0.85(A_{\text{c}} - A_{\text{core}}) \times \left(f'_{\text{cv}} \left[2\left(\frac{\varepsilon_{\text{c}}}{\varepsilon_{\text{cv}}}\right) - \left(\frac{\varepsilon_{\text{c}}}{\varepsilon_{\text{cv}}}\right)^2 \right]^{1/(1+2K_{\text{v}})} - \left(f^{\text{st}}_{\text{cv}} - f^{\text{cn}}_{\text{cv}}\right) \right) \tag{39}$$

$$K_{\text{v}} = \frac{k_{\text{l}} f_{\text{la,ev}}}{f'_{\text{co}}} \tag{40}$$

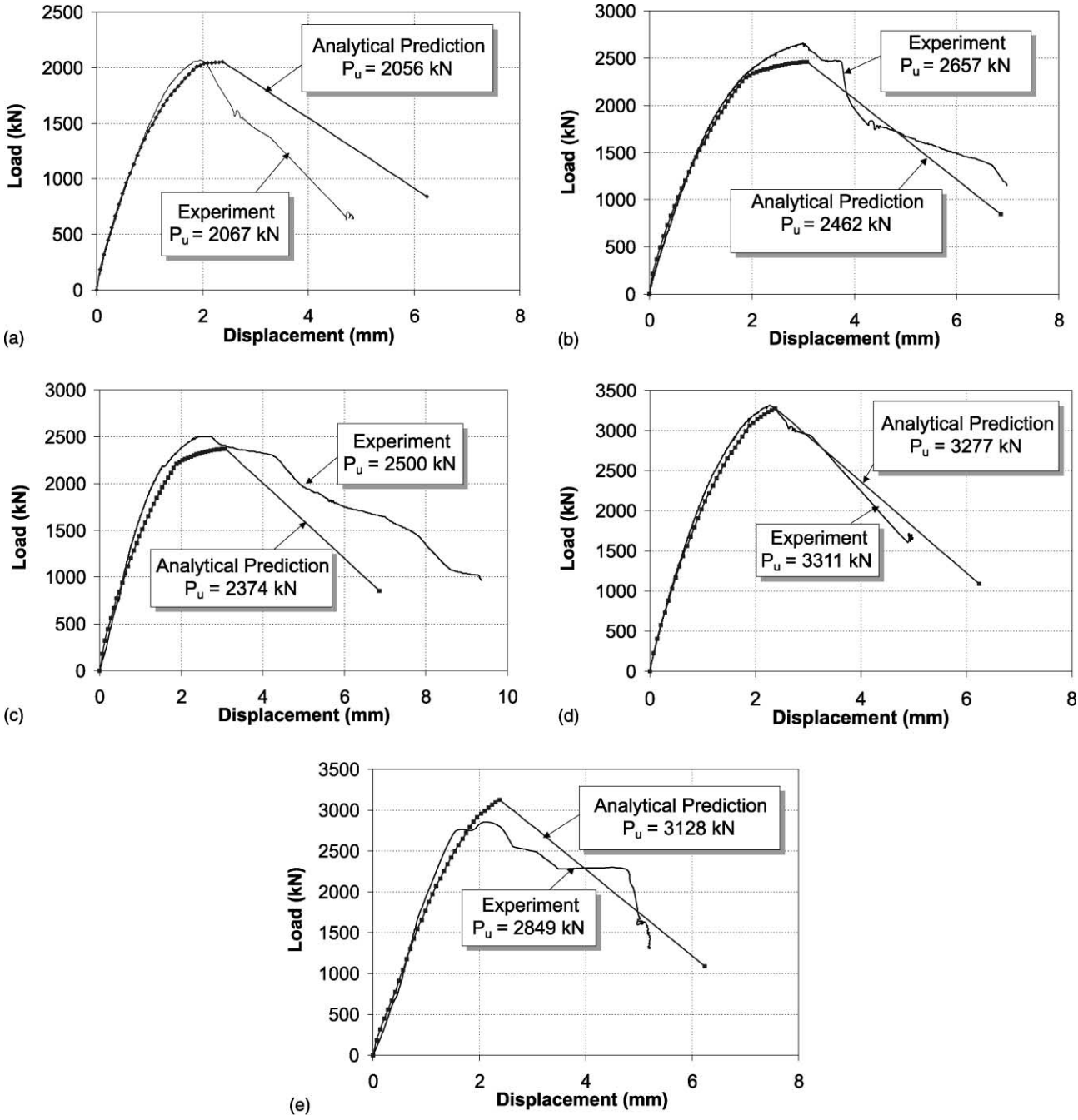

Fig. 9. Comparison between predicted and experimental load–displacement response of (a) control, (b) H2V-NL, (c) 2H2V-L, (d) 2H-VA-NL, and (e) 2H-VA-L.

Table 3
Comparison between predicted and measured peak load and displacement

Specimen	(a) Peak load (experiment) (kN)	(b) Displacement at peak load (experiment) (mm)	(c) Peak load (prediction) (kN)	(d) Displacement at peak load (prediction) (mm)	c/a	d/b
Control	2067	1.96	2050	2.38	0.992	1.214
2H2V-NL	2657	3.01	2462	3.08	0.927	1.023
2H2V-L	2504	2.43	2374	3.08	0.948	1.267
2H-VA-NL	3311	2.28	3277	2.38	0.990	1.044
2H-VA-L	2849	2.08	3128	2.38	1.098	1.144

where f'_{cv} and ε_{cv} are the confined cover concrete peak stress and strain, respectively, and $f_{la,ev}$ is the lateral confining pressure from the FRP wraps on the cover concrete.

4.4. Comparison between predicted and experimental esults

A comparison between the predicted and the measured load–displacement curves for all columns is shown in Fig. 9(a)–(e). A summary of the predicted and measured ultimate loads and displacements is given in Table 3. It can be seen that the load–displacement response given by the proposed model is in close agreement with the experimental results. The predicted ultimate load and displacement correlate well with the experimental results, with the latter being slightly overestimated. This may be due to the use of confinement coefficient k_2 originally derived for steel-confined concrete. A better prediction might be possible if the coefficient k_2 was obtained from experimental results of FRP-confined RC columns.

5. Parametric study

A parametric study was conducted using the proposed analytical model to investigate the effects of various parameters on the columns strengthening ratio (defined as the ultimate strength of a strengthened RC column divided by the ultimate strength of a control column). Among the parameters considered are the column's aspect ratio, the corner radius, the amount of vertical FRP (as percentage of cross-sectional area), and the number of horizontal FRP layers. Four different aspect ratios varying from 1:1 to 1:6 were investigated. In order to isolate the effects of each parameter, the compressive strength of the concrete, the ratio and strength of longitudinal and transverse reinforcement, the height of the column, the thickness of the concrete cover, and the spacing of the transverse reinforcement were all kept constant for all columns. A summary of the parametric study and the results obtained are given in Table 4 and Fig. 10(a)–(d), respectively.

It can clearly be seen from Fig. 10(a) that the column's aspect ratio has a significant impact on the strengthening ratio of the column. As the aspect ratio gradually increases from 1:1 to 1:6, the strengthening ratio reduces from 1.17 to 1.08—almost a 10% reduction. It is also interesting to note that as the column's aspect ratio increases, the reduction in the strengthening ratio becomes less and less significant. This is probably because passive confinement provided by the FRP (which controls the increase in axial-load carrying capacity) becomes less and less significant as the section aspect ratio continues to increase.

The effect of the number of horizontal FRP layers and the corner radius on the column's strengthening ratio is shown in Fig. 10(b) and (c), respectively. Both figures indicate that the column's strengthening ratio increases with the increasing number of horizontal FRP layers as well as with the increasing radius of the corner. However, the levels of increase depend on the column's aspect ratio. Columns with low aspect ratio experience much higher strength gain than columns with high aspect ratio.

The last parameter to be investigated was the effect of the percentage of vertical FRP reinforcement on the column's strengthening ratio. The result are shown in Fig. 10(d). It can be observed that, unlike other parameters, the increase in the strengthening ratio is similar for columns with different aspect ratios. This is because the contribution of this parameter to strength-

Table 4
Summary of the parametric study

Parameters	Range
Aspect ratio	1:1 (200 × 200 mm)
	1:2 (200 × 400 mm)
	1:4 (200 × 800 mm)
	1:6 (200 × 1200 mm)
Number of horizontal FRP layers	2
	4
	6
	8
Column's corner radius (mm)	15
	30
	45
Amount of vertical FRP (% of column's cross-sectional area)	0
	3
	6
	9

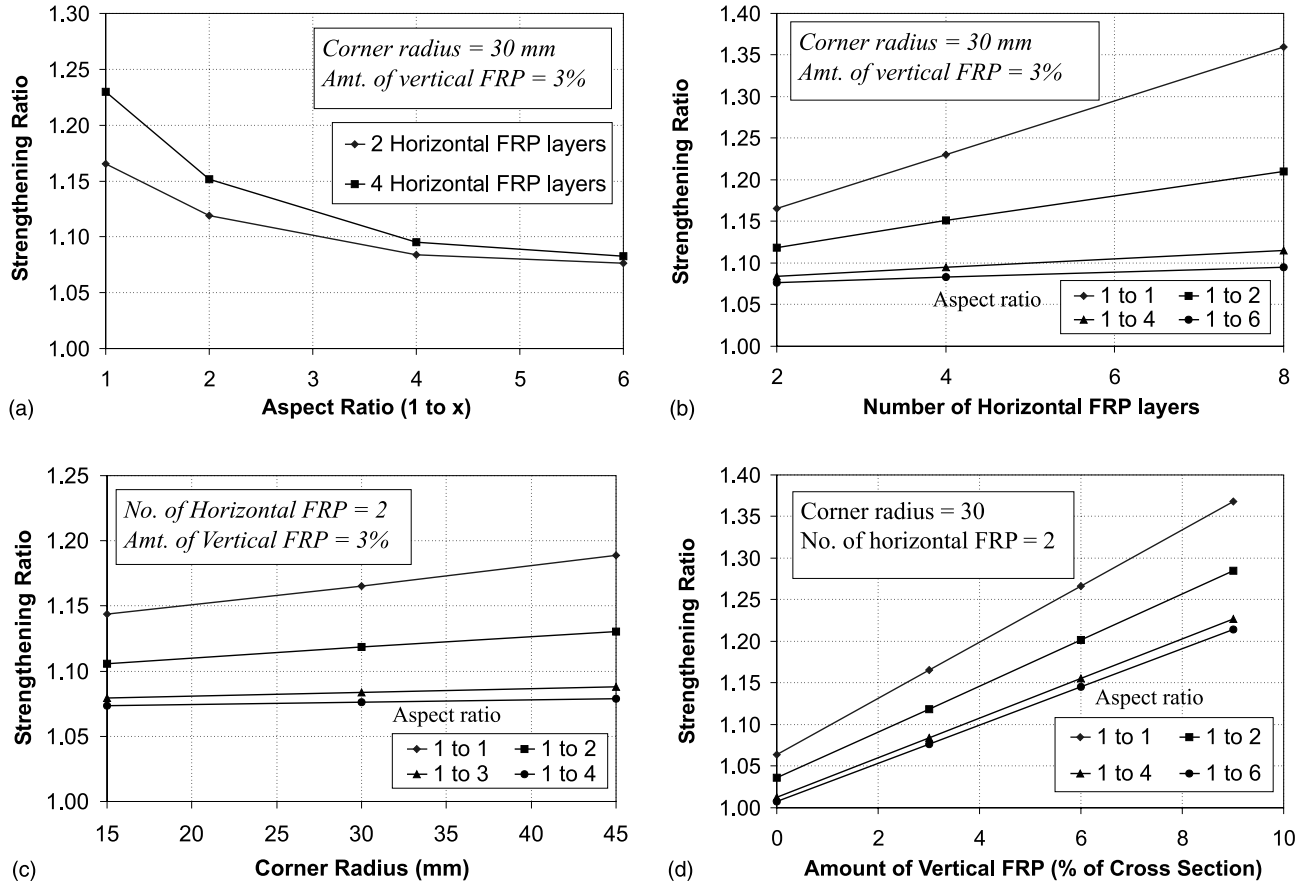

Fig. 10. Effects of (a) aspect ratio, (b) number of horizontal FRP layers, (c) column's corner radius, and (d) amount of vertical FRP on the strengthening ratio.

ening is independent of the passive confining pressure provided by the horizontal FRP wraps but depends on the column's perimeter. It can, therefore, be stated that in order to effectively strengthen columns with high aspect ratio, the strengthening scheme should focus on introducing more vertical reinforcement instead of more confining pressure. For columns with low aspect ratio, however, a strengthening scheme, which combines external confinement and vertical reinforcement, should be adopted to attain a high strengthening ratio.

6. Conclusions

An analytical model to predict the load–displacement response of wall-like RC columns strengthened with FRP wraps with and without sustained loading was presented. The load–displacement response determined from the analytical model was compared to the experimental results, and a close agreement has been observed. A parametric study on the important parameters governing the column's strengthening ratio was also presented. The following conclusions can further be drawn from the study:

1. The effect of sustained loading on the strengthening efficiency should be accounted for in the design of column strengthening schemes. More experimental studies are however required to fully correlate the strengthening ratio to various levels of sustained loading.
2. The steel-confined concrete model can be used to predict the ultimate load and displacement of wall-like RC columns strengthened with FRP wraps with and without sustained loading.
3. The parametric study shows that the column's aspect ratio, the number of horizontal FRP layers, the corner radius, and the amount of vertical FRP reinforcement are all important parameters which influence the strengthening ratio of FRP-wrapped RC columns.
4. The strengthening of columns with high aspect ratio should focus more on the introduction of extra vertical reinforcement rather than on confinement as the latter is less effective.

References

[1] Toutanji HA. Stress–strain characteristics of concrete columns externally confined with advanced fiber composites sheets. ACI Mater J 1999;96(3):397–404.

[2] Spoelstra MR, Monti G. FRP-confined concrete model. ASCE J Compos Construct 1999;3(3):143–50.

[3] Saadatmanesh H, Ehsani MR, Li MW. Strength and ductility of concrete columns externally reinforced with fiber composite straps. ACI Struct J 1994;91(4):434–47.

[4] Saadatmanesh H, Ehsani MR, Jin L. Repair of earthquake-damaged RC columns with FRP wraps. ACI Struct J 1997; 94(2):206–15.

[5] Mirmiran A, Shahawy M, Samaan M, Echary HE, Mastrapa JC, Pico O. Effect of column parameters on FRP-confined concrete. ASCE J Compos Construct 1998;2(4):175–85.

[6] Rochette P, Labossiere P. Axial testing of rectangular column models confined with composites. ASCE J Compos Construct 2000;4(3):129–36.

[7] Kaluarachchi DM. Performance of repaired axially-loaded members. MEng thesis. Singapore, National University of Singapore, 1997.

[8] Neale KW, Demers M, DeVino B, Ho NY. Strengthening of wall-type reinforced concrete columns with fibre reinforced composite sheets. In: Ong KC, Lau JM, Paramasivam P, editors. Proceedings of the Fifth International Conference on Structural Failure, Durability, and Retrofitting. Singapore: Singapore Concrete Institute; 1997. p. 410–7.

[9] Chiew SP, Lau JM, Ho NY. Testing of wall-type reinforced concrete column strengthening with advanced composite materials. In: Proceedings of a Seminar on Strengthening and Upgrading Structures Using Advanced Composite Materials. Singapore: Singapore Concrete Institute; 1999. p. 1–16.

[10] Tanwongsval S, Maalej M, Paramasivam P. Strengthening of RC wall-like columns. In: Malhotra VM, editor. Proceedings of the Fifth CANMET/ACI International Conference on Recent Advances in Concrete Technology, ACI SP-200. Detroit: American Concrete Institute; 2001. p. 663–76.

[11] Richart FE, Brandtzaeg A, Brown RL. Study of the failure of concrete under combined compressive stresses. Bulletin 185, University of Illinois Engineering Experiment Station, Champaign, 1928.

[12] Saatcioglu M, Razvi SR. Strength and ductility of confined concrete. ASCE J Struct Eng 1992;118(6):1590–607.

[13] Mander JB, Priestley MJN, Park R. Theoretical stress–strain model for confined concrete. ASCE J Struct Eng 1988; 114(8):1804–26.

[14] Popovics S. A numerical approach to the complete stress–strain curves for concrete under combined compressive stresses. Cement Concrete Res 1973;3(5):583–99.

[15] Sheikh SA, Uzumeri SM. Strength and ductility of tied concrete columns. ASCE J Struct Division 1980;105(5):1079–102.

[16] Hognestad E. A study of combined bending and axial load in reinforced concrete members. Bulletin 399, University of Illinois Engineering Experimental Station, Champaign, 1951.

[17] Ahmad SH, Shah SP. Stress–strain curves of concrete confined by spiral reinforcement. Proc, ACI J 1982;79(6):484–90.

[18] Pantazopoulou SJ, Mills RH. Microstructural aspects of the mechanical response of plain concrete. ACI Mater J 1995;92(6): 605–16.

[19] Yalcin C, Saatcioglu M. Inelastic analysis of reinforced concrete columns. Comput Struct 2000;77:539–55.